Colloid Polym Sci 276:434–442 (1998)

ORIGINAL CONTRIBUTION

H.-J. Jacobasch
F. Simon
P. Weidenhammer

Adsorption of ions onto polymer surfaces and its influence on zeta potential and adhesion phenomena

Received: 18 November 1997
Accepted: 19 January 1998

Prof. Dr. H.-J. Jacobasch†
F. Simon (✉) · P. Weidenhammer
Institute of Polymer Research Dresden
P.O. Box 120411
D-01005 Dresden
Germany

†Deceased.

Abstract The adhesion behavior that governs many technologically and biologically relevant polymer properties can be investigated by zeta potential measurements with varied electrolyte concentration or pH. In a previous work [1] it was found that the difference of the adsorption free energies of Cl^- and K^+ ions correlates with the adhesion force caused by van der Waals interactions, and that the decrease of adhesion strength by adsorption layers can be elucidated by zeta potential measurements. In order to confirm these interrelations, zeta potential measurements were combined with atomic force microscopy (AFM) measurements. Force–distance curves between poly(ether ether ketone) and fluorpolymers, respectively, and the Si_3N_4 tip of the AFM device in different electrolyte solutions were measured and analysed. The adsorption free energy of anions calculated from the Stern model correlates with their ability to prevent the adhesion between the polymer surface and the Si_3N_4 tip of the AFM device. These results demonstrate the influence of adsorption phenomena on the adhesion behavior of solids. The results obtained by AFM confirm the thesis that the electrical double layer of solid polymers in electrolyte solutions is governed by ion adsorption probably due to van der Waals interactions and that therefore van der Waals forces can be detected by zeta potential measurements.

Key words zeta potential – atomic force microscopy – X-ray photoelectron spectroscopy – adhesion – dispersion forces – ion adsorption

Introduction

Electrokinetic measurements are well established methods for elucidating colloid stability according to the DLVO theory and acid–base properties of solids or colloid particles [2, 3]. Furthermore, the adsorption thermodynamic and kinetic of surfactant, polyelectrolyte and protein adsorption onto different substances can be investigated [2–6].

Although Stern's double layer theory [7] considers the adsorption of small monovalent ions such as Cl^-, OH^-, etc. at the solid/electrolyte interface and its influence on electrokinetic phenomena less attention has been paid to the ion adsorption. A recent publication by Ninham and Yaminski [8] has pointed out that specific ion adsorption due to dispersion forces should not be neglected because it influences many phenomena in colloid and surface science such as conformation and solubility of electrolytes, flocculation, micelle formation, etc.

From this point of view, the origin of the electrical double layer on polymers without dissociable groups and the correlation between dispersion forces and ion adsorption will be discussed.

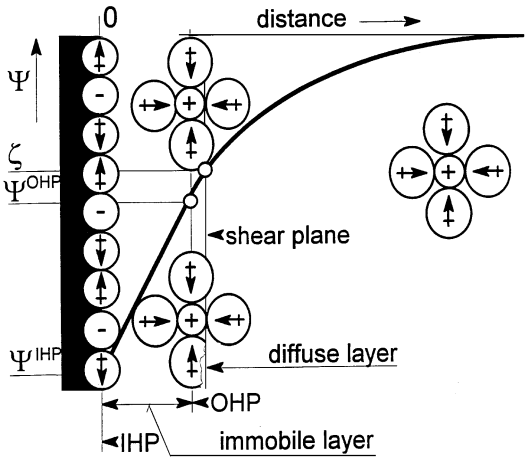

Fig. 1 The build-up of an electrical double layer according to Gouy–Chapman–Stern–Graham model

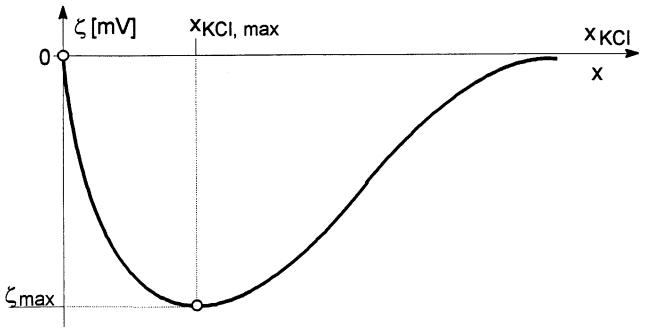

Fig. 2 Zeta potential of polymers as a function of KCl concentration

The zeta potential concept

The validity of the Gouy–Chapman–Stern–Graham model (GCSG) of the electrical double layer at the polymer/electrolyte interface can be considered as confirmed. The formation of the electrical double layer is mainly caused by dissociation of acidic or basic molecule groups and preferential adsorption of one kind of ions [2, 3].

According to the GCSG model the electrical double layer is divided into the inner (IHP) and outer (OHP) Helmholtz planes and the diffuse layer. In the electrokinetic experiment, an external force field is applied to the solid/liquid system and generates a relative movement of the liquid and the solid phase. This leads to a charge separation in the electrical double layer. Ions underlying a higher attractive force as the external force remains on the solid phase while charge carriers which are bounded more weakly move with the liquid phase. The zeta potential is the electrical potential of the shear plane, where the charge separation takes place (Fig. 1), relative to the bulk phase. Therefore, the zeta potential reflects the force balance between the external force and the interaction forces between ions and the solid surface. In other words, if the external force is known, the zeta potential allows to characterize the equilibrium between the ions in the electrolyte solution and at the solid surface.

If the polymer surface does not contain a native surface charge, it may however be charged by the preferential adsorption of anions or cations, respectively. Therefore, a non-zero zeta potential will be maesured. Also the surface potential may appear to be different from zero, as can be shown by direct force measurements for example. In this case, it is useful to define the plane of the surface potential at a distance δ away from the surface, where δ is the radius of the adsorbed ions. In the Stern model, the IHP is then represented by the adsorbed layer of potential determining ions.

Stern [7] predicted a parabolic function $\zeta = \zeta(x)$ for solids in contact with 1:1-electrolyte solutions, where x is the molar fraction of the electrolyte cations and anions (Fig. 2).

The shape of the function $\zeta = \zeta(x)$ predicted by Stern was confirmed by the electrokinetic investigations of many polymers (fibres or plates) by electro-osmosis and streaming potential measurements also when considering the surface conductivity [9–12]. However, different polymer latices characterized by electrophoresis did not show an extremum when the surface conductivity has been considered [13–15].

From the coordinates of the extremum $[x_{max}; \zeta_{max}]$ the molar adsorption free energies for monovalent anions Φ_- and cations Φ_+ can be calculated:

$$\Phi_- + \Phi_+ = 2R\,T \ln [x_{max}], \quad (1)$$

$$\Phi_- - \Phi_+ = 2F\,\zeta_{max}, \quad (2)$$

where R is the gas constant, T the absolute temperature, and F the Faraday constant.

The assumption that the extremum of the function $\zeta = \zeta(x)$ is caused by preferential anion adsorption due to dispersion interactions between the solid and the anions was supported by experiments that show that

- the value of ζ_{max} in KCl solution of poly(acrylonitril) fibres increases with increasing Hamaker constant of the fibres (varied by copolymerisation) and decreases with increasing porosity of the fibres (varied by spinning conditions) [1, 9, 16].
- there is a linear correlation between adhesion of fibres towards pigments and ζ_{max} in KCl solutions [9, 17].
- the changing of the adhesion behavior of polymers by adsorption layers can be described by zeta potential measurements [1, 9, 16].

The results reported above can be explained by the microscopic theory of dispersion forces. According to this theory the dispersion energy per area (E_{disp}) between two parallel plates is given by Eq. (3).

$$E_{disp} = -\frac{A}{12\pi d^2} = -\frac{\pi \beta q^2}{12 d^2}, \quad (3)$$

where A is the Hamaker constant, β the London constant, q the number of particles per unit volume, and d the distance between two parallel plates.

From this equation it is expected that the dispersion energy between solids and ions should be direct proportional to A and indirectly proportional to the solid's porosity which corresponds indirectly with the number of molecules per unit volume. This was confirmed experimentally for poly(acrylonitrile) fibres [1, 9, 18]. However, the uptake of colored pigment particles was detected with optical methods.

Nowadays it is possible to investigate adhesion forces (even between small particles) on a molecular level by direct force measurements, e.g. atomic force microscopy (AFM). The zeta potential of smooth polymer plates can be measured as well, and we are planning to use these techniques to give a more profound background to the rather phenomenological results obtained until now (see also [19, 20]).

Experimental

X-ray photoelectron spectroscopy

X-ray photoelectron spectra were recorded to get information about the chemical surface structure. An ESCAlab 220i (Fisons Instruments, East Grinstead, England) equipped with a non-monochromized Mg K_α X-ray source was used. The pass energies of the hemispheric analyser were constant with 80 eV for survey and 25 eV for high-resolved spectra. Peak fitting procedures were carried out after background subtraction according to Shirley [21]. Fit parameters were the position of the peak maximum, the full width at half maximum, the peak area, and the Gaussian–Lorentzian ratio. The elemental surface compositions were determined from the peak areas by using Wagner's sensitivity factors [22] and the spectrometer transmission function.

Electrokinetic experiments

All streaming potential measurements to determine the zeta potential values were carried out with the Electrokinetic Analyzer (Anton Paar KG, Graz, Austria) and the measuring cell for flat plates as described in Ref. [23].

Force measurements

An atomic force microscope (AFM, Digital Instruments, Santa Barbara, USA) was used to measure the forces between a Si_3N_4 probe, which is mounted on a cantilever spring, and the solid polymer surfaces in aqueous electrolyte solutions. The interaction forces between the sample and the Si_3N_4 tip cause a deflection of the cantilever. It is detected via a laser beam on a split photo diode (Fig. 3). Force–distance curves were obtained by recording the cantilever deflection (which equals the interaction force if multiplied by the spring constant) for a full extension–retraction cycle of the piezoelectric crystal which holds the sample (Fig. 4). During the approach cycle, a mechanical instability occurs when the gradient of the attractive force equals the cantilever spring constant, and the cantilever "jumps" into contact with the sample. This "jump-in" distance is therefore a measure for the reach of the net attractive interaction force. All force–distance curves shown in this paper are typical for the respective set of experiments.

The Si_3N_4 tip had been shown to have an isoelectric point $pH_{IEP} < 3$ [19]. Therefore, it is negatively charged in aqueous solutions with higher pH values. The pH_{IEP} of Si_3N_4 can vary from 2 to 9 [24], depending on the relative amount of Si–OH groups in comparison to basic silylamine groups on the surface. Obviously, the degree of oxidation is very high for the AFM probes used here. The surface potential of the Si_3N_4 probe can be regarded as constant in the electrolyte solutions which were used in this work.

Materials

Two different polymer materials without dissociable groups were chosen. A technical poly(ether ether ketone) (PEEK) (Victrex 450G, Victrex GmbH, Germany) with the chemical formula

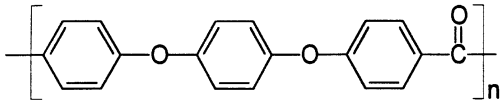

was injection moulded as plane sheets.

The fluorocarbon polymer was provided by the Institute for Applied Polymer Research, Teltow, Germany. It was plasma-deposited on a silicon wafer. After the

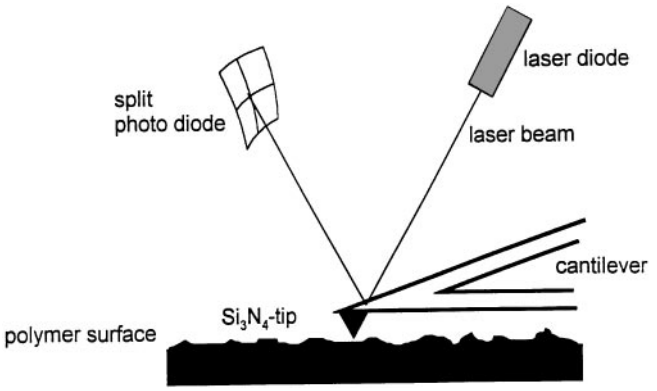

Fig. 3 Working principle of the atomic force microscope: the interaction forces between the sample and the Si_3N_4 probe cause a deflection of the cantilever. It is detected via a laser beam on a split photo diode

treatment the fluoronated silicon surface was very hydrophobic (advancing water contact angle: $\Theta_a = 116^\circ$).

Results and discussion

The survey X-ray photoelectron spectrum of PEEK is shown in Fig. 5a. Carbon, oxygen and traces of silicon were found in the surface region. The elemental ratio obtained from the survey spectrum $[O]:[C]_{XPS} = 0.1847$ agrees roughly with the theoretical ratio of the structure above ($[O]:[C]_{theo} = 3:19$). The difference between the theoretical and the measured ratio is conditional on the presence of silicon traces. The high-resolved C 1s spectrum shows three different component peaks which are expected from the formula above (Fig. 5b). Component peak *A* represents the $\underline{C}_xH_y$ species. This peak was used as reference peak to compensate electrostatic charging during the measurement. It was set on a binding energy of BE = 284.70 eV [25]. The second component peak *B* shifted to

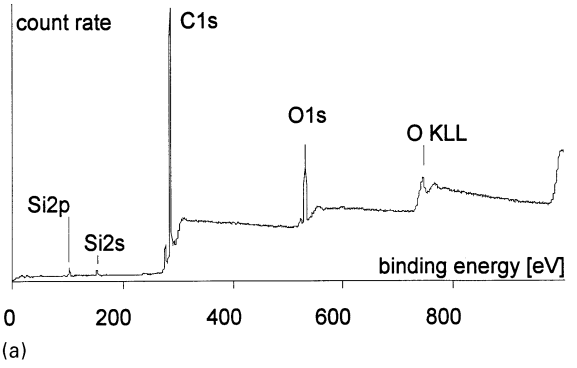

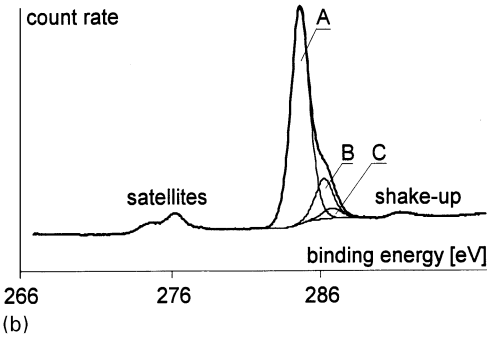

Fig. 5 (a) XPS spectrum of the poly(ether ether ketone) (PEEK). Traces of silicon are present, probably due to the silicon oil used to remove the polymer from the mould. (b) High-resolved C 1s spectrum of PEEK. Peaks that appear on a binding energies of 276 eV are satellites generates by Mg $K_{\alpha 3,4}$ X-rays

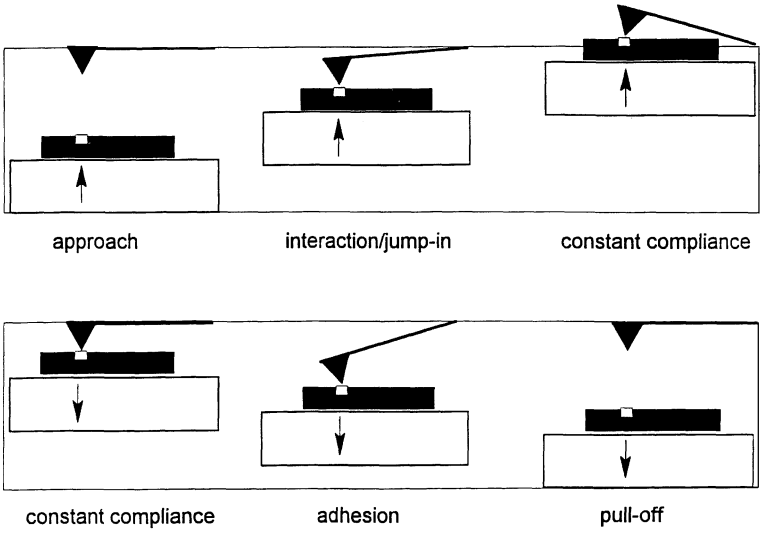

Fig. 4 Force–distance measurements in the AFM: tip and sample approach each other until contact and are drawn apart again. The interaction force is recorded by measuring the cantilever deflection continuously. The actual distance between tip and sample is calculated from the point of contact and the piezo travelling distance

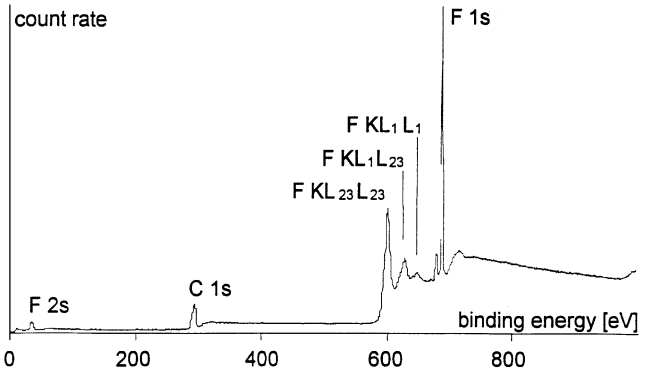

Fig. 6 XPS spectrum of the fluorocarbon polymer plasma-deposited to silicon wafer

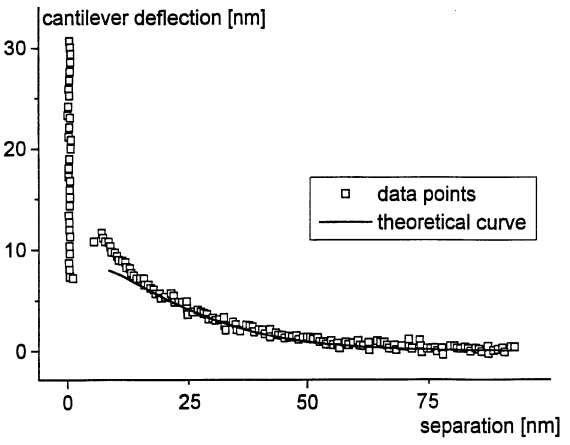

Fig. 7 Force–distance curve for PEEK and the Si_3N_4 AFM tip in a 0.3 mmoll^{-1} KCl solution, approach cycle. The parameters used for calculating the theoretical curve are explained in the text

higher binding energies (ΔBE = 1.48 eV) represents ether groups (C–O–C). Carbonyl groups are reflected by *C* at BE = 287.03 eV [26]. The ratio of the component peak areas $[A]:[B]:[C] = 16:4:1$ agrees with the expected theoretical ratio $[A]:[B]:[C] = 14:4:1$. Small differences found may be explained by siloxane and hydrocarbon impurities on the sample surface. The peak analysis of the C 1s spectrum shows that no carboxyl groups, which are able to dissociate, were found on the PEEK surface investigated.

Therefore, it can be concluded that there are no functional groups on the sample surface, which could cause a surface charge by dissociation in an aqueous environment.

The XPS spectrum of the fluorocarbon polymer is shown in Fig. 6. In the surface range, only fluorine and carbon were detected. The absence of oxygen, which would be part of carboxylic groups, implies that no dissociable groups are present on the sample surface.

Figure 7 shows the approach cycle of a force–distance curve between PEEK and the AFM tip in a KCl solution (3×10^{-4} moll^{-1}).

A long range electrostatic repulsion between the tip and the polymer sample is observed. The interaction force $F_{edl}(D)$ decreases exponentially with the distance *D*, the decay parameter is given by the inverse Debye length κ (see below). For long distances (down to 17 nm), the data are described by a theoretical curve calculated by using a linearized Poisson–Boltzmann equation and Derjaguin's approximation for dissimilar surface potentials [27]:

$$F_{edl}(D) = \pi r \varepsilon \kappa [(\psi_1^2 + \psi_2^2)(1 - \coth(\kappa D)) + 2\psi_1 \psi_2 \operatorname{cosech}(\kappa D)] , \quad (4)$$

where *D* is the separation distance, *r* the tip radius, ψ_1 and ψ_2 the surface potentials (which are meant to be constant during the interaction), κ the inverse Debye length and ε the electrical permittivity.

The Debye length depends on the valency and the concentration of the electrolyte ions and accounts for the screening of electrostatic potentials by the free charges in the electrolyte solution

$$\kappa^{-1} = \left(\sum_i \rho_{\infty i} e_0^2 z_i^2 / \varepsilon k T \right)^{-1/2} , \quad (5)$$

where $\rho_{\infty i}$ [m^{-3}] denotes the ion number density in the bulk electrolyte, e_0 the elementary charge, z_i the valency of ion *i*, $\varepsilon = \varepsilon_0 \varepsilon_r$ the electrical permittivity, and *k* the Boltzmann constant. At the distance κ^{-1} from a surface, the electrostatic potential is reduced to $1/e$ of its value on the surface.

Approaching the tip to the sample, at first a repulsive maximum occurs and at smaller distances attractive forces (electrostatic and van der Waals) govern the total interaction. Therefore, a "jump-in" is observed where the tip and the sample are coming into contact. During the retraction cycle (not shown in Fig. 7), a jump-out occurs, from which the pull-off force can be calculated using Hooke's law. If the area of contact is well known, the adhesion force can be determined via an appropriate contact mechanics model [28, 29].

The experimental data can be described by Eq. (4) using the following parameters, which were determined by a multiparameter fit of the data in Fig. 7:

Hamaker constant $A = 1 \times 10^{-20}$ J,
PEEK surface potential $\Psi_1 = -49$ mV,
tip surface potential $\Psi_2 = -55$ mV,
tip radius $r = 102$ nm,
Debye length $\kappa^{-1} = 15.1$ nm.

As shown by Eq. (4) the long range electrostatic interaction plays an important role for the adhesion of solids in aqueous media. Range and strength of the electrostatic interaction are determined by the surface potential and the Debye length.

Assuming that the zeta potential equals the surface potential, the electrostatic surface potential of the solid polymers investigated here also depends on the electrolyte concentration. Streaming potential measurements show the change of the surface potential with increasing electrolyte concentration. Using this method, an adsorption isotherm for the charge determining ions on the surface can be measured.

In Fig. 8 the function $\zeta = \zeta(x)$ curves are shown for PEEK, KCl, KOH, and Na_3PO_4, respectively. The polymer surface is charged negatively in all electrolytes, which means that the anions are adsorbed in excess on the surface [19]. The charging by OH^- and PO_4^{3-} ions is much stronger than by Cl^- ions. This results in different amounts of the surface potential, whose effects can be observed qualitatively in the force measurements (see below). The zeta potential measured in KCl at 0.3 mmol l^{-1} ($\zeta = -13$ mV) is much smaller than the surface potential $\Psi_1 = -49$ mV derived from the fit in Fig. 7. This discrepancy as well as the properties of the Si_3N_4 probe have to be a subject of further investigations.

If the surface potential is altered by the excess adsorption of the anion, the changes in the electrostatic interaction should be detectable by force–distance measurements with the AFM. An increase in the surface potential of the solid polymer leads to a decrease of the overall attractive interaction, if the tip surface potential is not altered. Figure 9 shows schematically the force–distance curves for different surface potentials, assuming interaction at constant potentials. The interaction forces (F_{total}) were calculated according to the DLVO theory, using Eq. (4) for the electrostatic interaction and an additive term representing the attractive dispersion contribution for a sphere of radius r and a flat plate with the Hamaker constant A:

$$F_{\text{total}}(D) = F_{\text{vdW}}(D) + F_{\text{edl}}(D) \tag{6}$$

with

$$F_{\text{vdW}}(D) = -\frac{Ar}{6D}\,. \tag{7}$$

In the following we assume that the Hamaker constant is not altered by the adsorption of ions. The validity of this first order approximation has to be discussed in detail in further work.

Figure 9 shows that an increase in the sample surface potential alters the force–distance curve significantly. Under the assumption that the interaction takes place at constant surface potentials, the electrostatic interaction

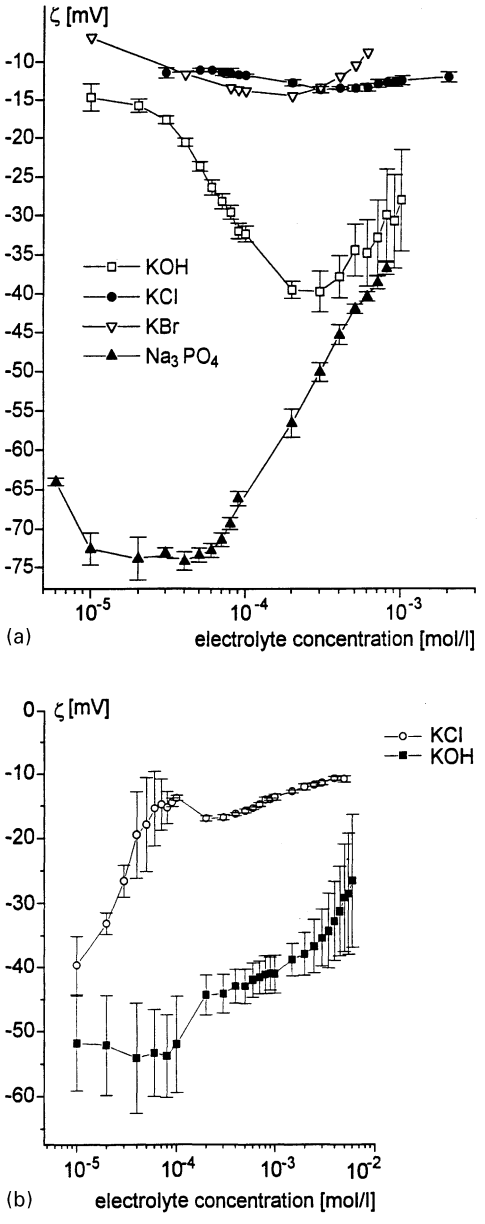

Fig. 8 Zeta potential of PEEK and the fluorocarbon polymer in dependence of the electrolyte concentration. (a) The PEEK is charged with increasing KOH, KCl, KBr and Na_3PO_4 concentrations. The zeta potential (and therefore the surface potential) in KCl and KBr is much lower than in KOH, but has an extremum in all electrolytes. The extremum in Na_3PO_4 is much more pronounced and occurs at lower concentrations than in the 1:1 electrolytes. For higher electrolyte concentrations, the zeta potential decreases due to double layer compression. (b) The fluorocarbon polymer is charged in the KOH solution. The presence of Cl^- ions, however, does not result in a more negative surface potential. The initial negative values at low concentrations are the same for both electrolytes, because the OH^- concentration in pure Millipore water due to autodissociation is identical

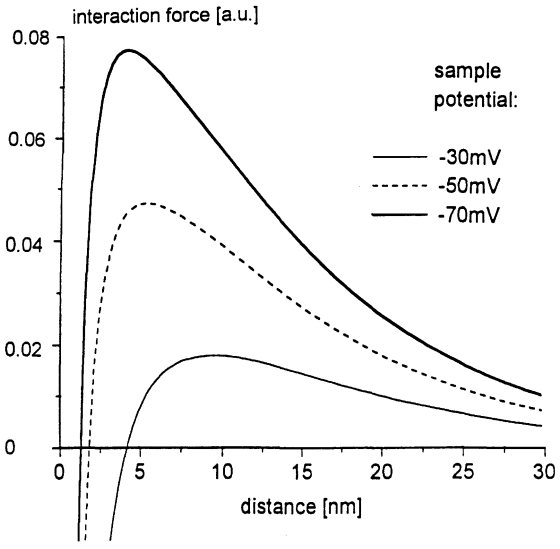

Fig. 9 Schematic force–distance curves for a sphere-plate system with different surface potentials in a 1 mmol l^{-1} monovalent electrolyte solution. A constant tip potential of -70 mV and a Hamaker constant of 10^{-20} J were assumed. The curves were calculated using a linearized Poisson–Boltzmann equation and the Derjaguin approximation [11]. Under the assumption that the interaction takes place at constant surface potentials, the electrostatic interaction turns from repulsive to attractive at a certain distance. This "jump-in" distance decreases with increasing surface potential

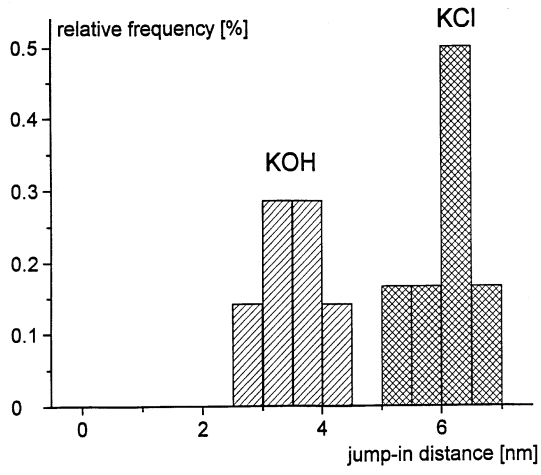

Fig. 10 Frequency distribution of "jump-in" distances between PEEK and the Si_3N_4 tip in 0.3 mmol l^{-1} KOH and KCl solution, respectively. The average jump-in distance in KOH is 3 nm, in KCl 6 nm

turns from repulsive to attractive at a certain tip–sample distance. The height of the repulsive barrier is increased with growing surface potential and its position is shifted towards the surface. Experimentally, that means that the jump-in distance is reduced for higher surface potentials. It cannot be proved that the surface potentials of our polymer surfaces remain constant during the interaction. In [30] it is pointed out that this assumption is often made for mathematincal convenience. It was shown that the constant potential limit gives a reasonable fit for experimental AFM force data measured on polypropylene surfaces [31]. Since the polymers investigated here do not contain dissociable surface groups either, this assumption seems reasonable here, too.

In Fig. 10, the jump-in distances for the Si_3N_4-PEEK system are shown in 0.3 mmol l^{-1} KOH and KCl solution, respectively. The KOH experiment shows a smaller reach of attraction than the KCl experiment. This is exactly what one would expect from the schematic force–distance curves in Fig. 9 since the PEEK surface potential in KOH is much larger than in KCl. If the electrolyte concentrations are increased, the jump-in distance is becoming smaller and smaller. At a concentration of 0.5 mmol l^{-1}, the attractive interaction disappears completely. This effect cannot be accounted for by the DLVO approximation for the electrostatic forces. For such small distances (<1 nm), additional effects, such as ion-correlation forces or finite ion-size effects are becoming important and can determine the behavior of the system [32].

However, the basic step is the preferential adsorption of anions which can be detected by zeta potential measurements.

For the fluorocarbon polymer, the situation is similar. The zeta potential increases with increasing KOH concentration but decreases with increasing KCl concentration [19]. Consequently, the position of the electrostatic repulsive barrier (Fig. 9) and therefore the jump-in distance decreases in KOH and increases in KCl solution (Fig. 11). The fact that there is no Cl^- adsorption at the fluorocarbon surface may be due to its low surface free energy.

The results show that the formation of electrical double layers is due to non-electrostatic adsorption of anions and can prevent adhesion.

In Table 1 the results of zeta potential and force measurements published partially in [19] are summarized. The difference of the anion and cation adsorption free energies were calculated from the extremum of the functions $\zeta = \zeta(x)$ using Stern's Eqs. (1) and (2).

Figure 12 shows the influence of the electrolyte concentration on the jump-out distance measured in the AFM experiments between Si_3N_4 and PEEK.

It is evident that the attraction between the polymer and the Si_3N_4 tip is lower, the higher the adsorption free energy of the anion. The electrolyte concentration which prevents adhesion corresponds roughly with the concentration at which the maximum zeta potential occurs (see Table 1). This value corresponds with a monolayer coverage. Therefore we can conclude that a monolayer of adsorbed ions can prevent adhesion.

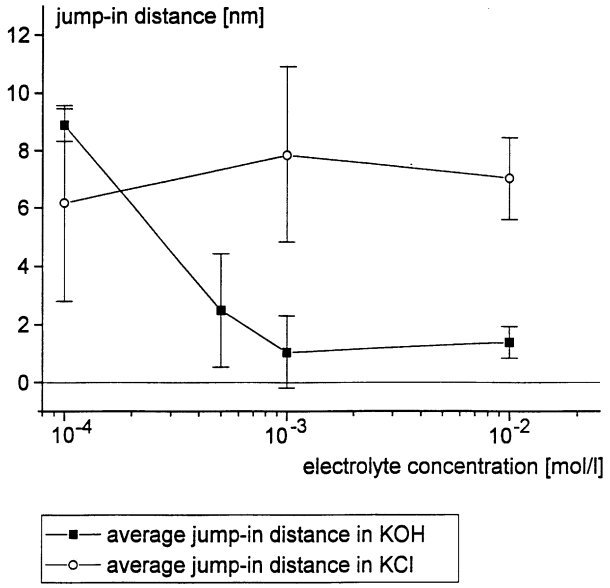

Fig. 11 "Jump-in" distance between the fluorocarbon polymer surface and the Si_3N_4 tip in dependence of the KOH and KCl electrolyte solution, respectively. Each data point was averaged over at least 20 force curves from different experimental runs using the same tip and cantilever, but different spots on the sample. The error bars show the standard deviation of the values

In a subsequent paper we will discuss some examples which show that this conclusion can be generalized for the adhesion in a number of systems [33].

Conclusions

From the results obtained by AFM measurements we can conclude the following: the solid polymers investigated here do not have a "native" surface potential in aqueous solutions, because they do not contain dissociable surface groups. However, in the direct force experiments, a negative electrostatic surface potential is observed, which must be due to the excess adsorption of anions from the electrolyte solution. Therefore, an electrical double layer is formed next to the solid polymer surface.

Zeta potential measurements can be used to measure the "adsorption isotherm" of ions on the solid polymer surface. The results can be taken as a measure for the surface potential. They are qualitatively in good agreement with the results from force–distance measurements in the respective electrolyte solutions. The dependence of the electrostatic interaction on the surface potential of the sample, which is expected from the theory of heterocoagulation, can be observed experimentally. The ion adsorption on primarily uncharged polymers can be explained by dispersion interaction as described by Ninham and Yaminski [8].

Table 1 Critical concentration values from zeta potential and force measurements: extremum zeta potential values ζ_{ex} and c_{ex}, excess anion adsorption free energy $|\Phi_- - \Phi_+|$ and the electrolyte concentration $c_{no\ jump}$, which prevents a jump into contact. $c_{no\ jump}$ is roughly in accordance with c_{ex}, where there is a monolayer coverage of ions on the solid surface. For CHF in KOH there is a significant discrepancy, which cannot be explained at the moment. For PEEK in KBr the error of $c_{no\ jump}$ is still large, because the number of experiments is not yet sufficient

Polymer	Electrolyte	ζ_{ex} [mV]	c_{ex} [mmol/l]	$\lvert\Phi_- - \Phi_+\rvert$ [kJ/mol]	$c_{no\ jump}$ [mmol/l]
PEEK	KOH	− 40	0.25	7.6	0.5
PEEK	KCl	− 14	0.45	2.6	0.5
PEEK	KBr	− 15	0.20	2.8	1
PEEK	Na_3PO_4	− 74	0.03		0.05

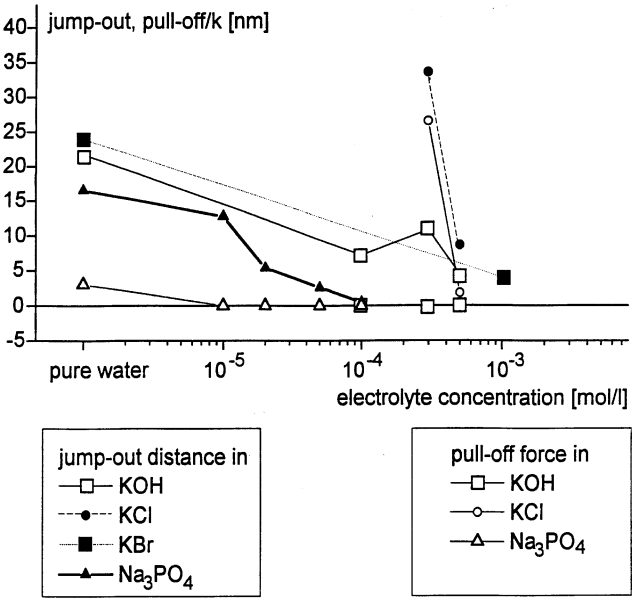

Fig. 12 "Jump-out" distances and pull-off forces between Si_3N_4 and PEEK in different electrolyte solutions with varying concentration. Each data point shows the average of at least 10 force–distance curves. The jump-out-distance (black symbols) indicates a minimum in the force–distance-curve, which is not necessarily attractive. The pull-off force (grey symbols) denotes the attractive force between the surfaces in contact, which has to be overcome in order to separate them again

From all these results we can see that zeta potential measurements in combination with force measurements can contribute to the understanding of adhesion phenomena.

Acknowledgements The authors thank Dr. J. Behnisch, Fraunhofer-Gesellschaft, Institute for Applied Polymer Research, Teltow, Germany for providing the fluorocarbon film. This work was supported by the Deutsche Forschungsgemeinschaft and the Max-Buchner Foundation.

References

1. Jacobasch HJ, Grundke K, Schneider S, Simon F (1995) J Adhesion 48:57–73
2. Lyklema J (1995) Fundamentals of Interface and Colloid Science, Vol 2: Solid–liquid interfaces. Academic Press, London
3. Hunter RJ (1981) Zeta Potential in Colloid Science: Principles and Applications. Academic Press, New York
4. Jacobasch HJ (1989) In: Mittal KL (ed) Surfactants in Solution, Vol. 9. Plenum Press, New York, pp 381–396
5. Elgersma AV, Zsom RLJ, Lyklema J, Norde W (1992) Colloids and Surfaces 65:17–28
6. Shirahama H, Lyklema J, Norde W (1990) J Colloid Interface Sci 139: 177–187
7. Stern O (1924) Zeitschrift für Elektrochemie 30:508–516
8. Ninham BW, Yaminski V (1997) Langmuir 13:2097–2108
9. Jacobasch HJ (1984) Oberflächenchemie faserbildender Polymerer. Akademie-Verlag, Berlin
10. Tasaka M, Tamura S, Takemura N (1984) J Memb Sci 12:169–182
11. Stackelberg M, Kling W, Benzel W, Wilke F (1954) Kolloid Z 135:67–80
12. Börner M, Jacobasch HJ, Simon F, Churaev NV, Segeeva IP, Sobolev VD (1994) Coll Surfaces A 85:9–17
13. Sonntag H (1977) Lehrbuch der Kolloidwissenschaft, Deutscher Verlag der Wissenschaften, Berlin
14. Van der Linde AJ, Bijsterbosch BH (1989) Colloids and Surfaces 41:345–352
15. Midmore BR, Hunter RJ (1988) J Colloid Interface Sci 122:521–529
16. Jacobasch HJ (1977) Das Papier 31:436–441
17. Flath HJ, Saleh N (1980) Acta Polymerica 31:510–517
18. Jacobasch HJ (1970) Textilveredlung 5:385–391
19. Weidenhammer P, Jacobasch HJ (1996) J Colloid Interface Sci 180:232
20. Weidenhammer P, Jacobasch HJ (1996) Polymer Preprints 37:614–615
21. Shirley DA (1972) Phys Rev B 5: 4709–4714
22. Wagner CD, Davis LE, Zeller MW, Taylor JA, Raymond RH, Gale LH (1981) Surface Interface Anal 3:211–225
23. Grundke K, Jacobasch HJ, Simon F, Schneider S (1995) J Adhesion Sci Technol 9:327–350
24. Greil P, Nitzsche R, Friedrich H, Hermel W (1991) J Europ Ceramic Soc 7:353–359
25. Beamson G, Briggs D (1992) High Resolution XPS of Organic Polymers. Wiley, Chichester, pp 172–173
26. Pawson DJ, Ameen AP, Short RD, Denison P, Jones FR (1992) Surf Interface Anal 18:13–22
27. Hunter RJ (1986) Foundations of Colloid Sciences, Vol 1. Clarendon Press, Oxford
28. Johnson KL, Kendall K, Roberts AD (1971) Proc R Soc London A 324: 301–313
29. Derjaguin BV, Muller VM, Toporov YP (1975) J Colloid Interface Sci 53:314–326
30. Atkins DT, Pashley RM (1993) Langmuir 9:2232–2236
31. Meagher L, Pashley RM (1995) Langmuir 11:4019–4024
32. Israelachvili JN (1992) Intermolecular and Surface Forces. Academic Press, London
33. Jacobasch HJ, Simon F, Weidenhammer P, in preparation